

## Shear capacity equation for channel shear connectors in steel-concrete composite beams

Masoud Paknahad <sup>\*1</sup>, Mahdi Shariati <sup>\*\*2,3,4</sup>, Yadollah Sedghi <sup>5</sup>,  
Mohammad Bazzaz <sup>6</sup> and Majid Khorami <sup>7</sup>

<sup>1</sup> Department of Civil Engineering, Mahallat Institute of Higher Education, Mahallat, Iran

<sup>2</sup> Faculty of Civil Engineering, University of Tabriz, Tabriz, Iran

<sup>3</sup> Malaysia-Japan International Institute of Technology, Universiti Teknologi Malaysia, Kuala Lumpur, Malaysia

<sup>4</sup> Department of Civil Engineering, University of Malaya, 50603, Kuala Lumpur, Malaysia

<sup>5</sup> Department of Civil Engineering, Qeshm International Branch, Islamic Azad University, Qeshm, Iran

<sup>6</sup> Department of Civil, Environmental, and Architectural Engineering, University of Kansas, Lawrence, KS, USA

<sup>7</sup> Facultad de Arquitectura y Urbanismo, Universidad Tecnológica Equinoccial, Calle Rumipamba s/n y Bourgeois, Quito, Ecuador

(Received March 22, 2018, Revised May 2, 2018, Accepted June 11, 2018)

**Abstract.** In this research the effect of high strength concrete (HSC) on shear capability of the channel shear connectors (CSC) in the steel concrete composite floor system was estimated experimentally and analytically. The push-out test was carried out for assessing the accurateness of the proposed model (nonlinear and finite element model) for the test specimens. A parametric analysis was conducted for predicting the shear capacity of the connectors (CSC) in the HSC. Eight push-out specimens of different sizes of channels with different high strength concrete were tested under the monotonic loading system. The aim of this study was to evaluate the efficacy of the National Building Code of Canada (NBC) of Canada for analysing the loading abilities of the CSC in the HSC. Using the experimental tests results and verifying the finite element results with them, it was then confirmed by the extended parametric studies that the Canadian Design Code was less efficient for predicting the capacity of the CSC in the HSC. Hence, an alternative equation was formulated for predicting the shear capacity of these connectors during the inclusion of HSC for designing the codes.

**Keywords:** high strength concrete; channel shear connector; push-out test; finite element analysis; steel concrete composite floor

### 1. Introduction

There are innovative passive control systems to prevent the failure of steel structures by preventing the buckling of bracing systems and dissipating the earthquake energy in a circular element (Andalib *et al.* 2010, 2011, 2014, 2018, Bazzaz 2010, Andalib 2011, Bazzaz *et al.* 2011a, Heydari 2011, Bazzaz *et al.* 2012a, 2014, 2015a).

Also, there are some investigation on the behavior of the columns under seismic events such as buckling-controlled braces (BCBs) with various cross sections, Reduced Web Section (RWS) connection with rectangular web opening, and special concentrically braced frames (SCBFs) (Kazemi *et al.* 2012, Momenzadeh 2012, Momenzadeh *et al.* 2017a, Shen *et al.* 2017, Heydari and Shariati 2018, Momenzadeh and Shen 2018). Furthermore, according to works of Rassouli *et al.* (2016), using steel-concrete composite structures provides higher lateral stiffness, strength, energy absorption, and ductility for high-rise buildings designed in

region of high seismic hazard (Rassouli *et al.* 2016, Shafaei *et al.* 2016, Shafaei *et al.* 2017, 2018). Moreover, mechanical shear connectors are commonly used to transfer longitudinal shear forces across the steel-concrete interface in steel concrete steel-concrete composite beams.

The application of the CSC alternative to the conventional shear connectors (studs) turns out to be a good option (Maleki and Mahoutian 2009). Among the advantages of shear connectors, the most noticeable are the higher loading capacity, reliable for conventional welding system, and simple assessment process which does not require the bending test designed for stud connectors. Therefore, few CSC required for an assembly than the conventional headed stud shear connectors (Maleki and Bagheri 2008a, Abedini *et al.* 2017). Several researchers (Hosain and Pashan 2006, Maleki and Bagheri 2008b, Hosain and Pashan 2009, Baran and Topkaya 2012, Shariati *et al.* 2012b, Baran and Topkaya 2014, Toghroli *et al.* 2014, Fanaie *et al.* 2015, Shahabi *et al.* 2016, Shariati *et al.* 2016, Safa *et al.* 2016) had analysed preliminary test results of the CSC for classifying the behaviour of these connectors. They also analysed the test results for evaluating the probability and suitability of the profiles (channel profiles) as the connectors. Based on previous studies, several equations were formulated for getting desired capacity of the CSC in the solid concrete slab using different building codes

\*Corresponding author, Ph.D.,

E-mail: [mpaknahad@mahallat.ac.ir](mailto:mpaknahad@mahallat.ac.ir)

\*\*Ph.D., E-mail: [mahdishariati@utm.my](mailto:mahdishariati@utm.my);

[shariatimehdi@yahoo.com](mailto:shariatimehdi@yahoo.com)

Table 1 The geometrical properties of the channel utilised for this experiment

Specimen	Height (mm)	Length (mm)	Web thickness (mm)	Flange thickness (mm)
10050	100	50	6	8.5
7550	75	50	5	7.5
10030	100	30	6	8.5
7530	75	30	5	7.5

{National Building Code of Canada (NBC) (NBC 2005) and Code of the American Institute of Steel Construction (AISC)} (AISC 2005). Maleki and Bagheri (2008a) recently conducted some tests for evaluating the strength of the connectors (channel connectors) implanted in concrete materials by two types of loading system (monotonic and fatigue loading system). The slabs were included engineered cementitious composite along with several types of concretes such as the plain, fibre reinforced, and reinforced concrete. Furthermore, Maleki and Mahoutian (Maleki and Mahoutian 2009) had suggested a modified equation for predicting the capacity of the CSC surrounded in the polypropylene concrete whereby Shariati *et al.* (2010, 2011) recommended the embedment in the light-weight aggregate concrete (LWAC).

Previously, two equations were suggested by Pashan and Hosain (Hosain and Pashan 2009) for estimating the capacity of the channel in the solid and metal deck slabs. However, the NBC code (NBC 2005) was observed to be the most consistent code for getting desired shear capacity of a CSC embedded in the solid slab (Eq. (1)) as follows

$$Q_n = 36.5 \times (t_f + 0.5t_w) \times L_c \times \sqrt{f_c} \quad (1)$$

Where,  $Q_n$  represents the strength of CSC (N),  $t_f$  denote the thickness of flange (mm),  $t_w$  exhibit thickness of the web (mm),  $L_c$  is the length (mm), and  $f_c$  represents the compressive strength of concrete (MPa). Uses of the HSC in composite construction facilitate more slender structures and higher loading capacity along with the durability and strength than the normal concrete (Mohammadhassani *et al.* 2013, Awal *et al.* 2015). Besides, it (HSC) helps to change the ratio (maximum slip requirement and connection deformation capacity ratio) significantly but requires direct connection with the ductility. Furthermore, the HSC helps to produce cost-effective products with the reasonable technical solution (Akgul *et al.* 2017). The application of the HSC in a composite beam requires the specific ductility properties, load carrying capacities and the fatigue behaviour. Therefore, uses of the HSC in composite beams in combination with the channel and stud shear connectors become a common procedure. However, the push-out tests for the normal and HSC were assessed, but a limited study reported the behaviour of the connectors in the HSC. Hence, this testing procedure seems to be more promising and interesting for studying the behaviour of the CSC in the HSC.

In previous experiments, the finite element analysis (FEA) was used as an analytical tool for studying the behaviour of the composite beams (Ayatollahi *et al.* 2011, Shafieifar *et al.* 2016, Abedini *et al.* 2017, Bozorgzad and

Lee 2017, Farzad *et al.* 2017, Haji Agha Mohammad Zarbaf *et al.* 2017a, Shafieifar *et al.* 2017). The results and analyses of these experiments need to verify and compare the accurate test results. The connectors (steel part) and the slab (concrete part) were utilised for the three-dimensional and nonlinear performance of the push out specimens (Eslami and Namba 2016a, b, c, Shafaei *et al.* 2016, Haji Agha Mohammad Zarbaf, Norouzi *et al.* 2017a, b, Kodur *et al.* 2017). This phenomenon caused the mathematical modelling very complicated. However, these types of interactions were considered in the comprehensive FEA of the shear connectors and described elaborately in the literature.

In this experiment, consequences of monotonic push-out test on the normal and high strength reinforced concrete were investigated, and their results were reported. These results were also being applied for calibrating a proposed model (nonlinear finite element model). The calibration of a model using parametric study was conducted for getting an equation for predicting the ultimate capacity of the CSC embedded in the HSC.

## 2. Research methodology

### 2.1 Experimental procedure

#### 2.1.1 Details of the specimen and setup test

The strength and size of the CSC were assessed in eight push-out specimens using the concrete slabs. Among the eight specimens, four specimens were examined using the monotonic loading system in the high strength reinforced concrete while the other four specimens were investigated using the normal weight concrete. In this experiment, the push-out specimens consist of a steel I-beam with two slabs attached to each flange. Besides, each flange was welded on the channel while layers of steel bars (two layers) and four steel bar hoops (10 mm diameter) were placed in two perpendicular directions on all slabs. These four types of channels which were 100 and 75 mm height and 30 and 50 mm long were used in this experiment. The high channels (100 mm) contained a flange (6 mm thick) with the web thickness of 8.5 mm while the 75 mm channels possessed flange thickness of 5 mm with the web thickness of 7.5 mm. The geometrical properties of the channel which were used for the tests are depicted in Table 1 as below.

The compression strength of the normal reinforced concrete was considered as 38.2 MPa which was expected to be 63 and 82 MPa as in the HSC. The compressive strength of HSC varied in between 41 and 82 MPa as mentioned in the ACI 363. However, as the chosen levels of HSC were within the range (41 to 82 MPa) so these two

levels of HSC were the representative of the HSC. The compressive strength of the normal concrete was determined using cube and cylinder tests of the samples while the strength of normal concrete was observed higher than the cylinder samples (Toghroli *et al.* 2018). In this experiment, the concrete cubes (100 mm) were employed as standard specimens for measuring the compressive strength as stated in the British Standard Code. Conversely, the uses of concrete cylinders (150×300 mm) were proposed by the American Standard Code. The cube samples which were used in this investigation exhibited a higher compressive strength due to different geometrical shapes of the samples (aspect ratio) as well as due to the end effect of the machine plates. However, the strength (compressive strength) of the cylinder samples was lower (5% to 25%) than the strength of cube samples. The differences between the cube and cylinder samples inversely depended on the concrete strength. A factor (1.2 as BS 1881: Part120 (BSI 1983)) was employed for the conversion of strength (compressive strength) of cylinder samples to cube samples in the normal strength concrete. The cylinder and cube samples were tested during this study as stated on the ASTM C39 (ASTM 2005) and BS 1881 (BS 1881 1983) for compressive strength measurements. The results of the compressive

strength were an average of the samples while the shape factor of 1.2 (BS1881 (BSI 1983)) was used only for the cylinder samples. The air-dry condition was used for aggregates of both types of HSC mixes where the fine aggregate was graded as the silica sands with the maximum size of 4.75 mm and the coarse aggregate was graded as the crushed granite with the maximum size of 10 mm. The particle size of the fine aggregate is shown in Table 2 (Sajedi and Abdul Razak 2010). The Ordinary Portland Cement (OPC) corresponded to the type II ASTM C150 (Cement) were utilised and their chemical properties are shown in Table 3 (Razak and Sajedi 2011). Moreover, the super plasticiser (SP) was used for achieving an acceptable workability in both mixes. The SP was named as Rheobuild 1100 possessed the gravity of approximately 1.195, and dark brown colour with a pH range of 6.0-9.0 (Sajedi and Razak 2011). Properties of concrete materials are exhibited in Table 4. Short lengths of the channels were used because of the size limitation of the concrete slab. All push-out specimens were casted in the horizontal position where a reliable quality of concrete was also assumed. All specimens had been cured under water for 28 days before testing, where all samples were cured until the testing day. The mixing proportion of concrete for all specimens is

Table 2 The particle sizes of the silica sand (SS) according to the BS 822: Clause 11

Sieve size ( $\mu\text{m}$ )	Sieve No.	$W_{SS}+W_S$ (g)	$W_S$ (g)	$W_{SS}$ (g)	Ret.%	Cum.Ret.%	Pass %
4750	3/16 in	409.9	408.3	1.6	0.32	0.032	99.68
2360	NO.7	462.3	375.7	86.6	17.33	17.65	82.35
1180	NO.14	437.2	343.0	94.2	18.85	36.5	63.50
600	NO.25	450.7	316.2	134.5	26.93	63.42	36.58
300	NO.52	379.1	288.7	90.4	18.09	81.51	18.49
150	NO.100	322.1	274.8	47.3	9.47	90.99	9.02
75	NO.200	309.9	275.2	34.7	6.94	97.92	2.08
Pan	-	250.8	240.4	10.4	2.08	-	0.00
Total				499.7		388.31	

\*Fineness modulus =  $388.31/100 = 3.88$ ; Water absorption for silica sand is 0.93%; WSS = Silica sand weight; WS = Sieve weight; Cum. Ret = Cumulative retained

Table 3 Distribution of grain size for the granite gravels according to the Standard (1992)

Sieve size ( $\mu\text{m}$ )	Sieve size (in)	$W_G+W_S$ (g)	$W_S$ (g)	$W_G$ (g)	Ret.%	Cum.Ret.%	Pass %
19	3/4	1626.6	1616.1	10.5	0.42	0.42	99.58
12.7	1/2	2181.6	1398.8	782.8	31.32	31.74	68.26
9.5	3/8	2271.3	1378.4	892.9	35.72	67.46	32.54
4.75	3/16	2170.5	1397.4	773.1	30.93	98.39	1.61
Pan	-----	886.2	846.0	40.2	1.61	-----	0.00
Total				2499.5	100	600+198.01	

Table 4 The composition of cementitious materials in OPC (% mass)

$\text{P}_2\text{O}_5$	$\text{SiO}_2$	$\text{Al}_2\text{O}_3$	MgO	$\text{Fe}_2\text{O}_3$	CaO	MnO	$\text{K}_2\text{O}$	$\text{TiO}_2$	$\text{SO}_3$	$\text{CO}_2$	LOI
0.068	18.47	4.27	2.08	2.064	64.09	0.045	0.281	0.103	4.25	4.20	1.53

Table 5 The mixing proportions of the HSC materials by weight

Mix no.	Cement (kg/m <sup>3</sup> )	Coarse aggregate (kg/m <sup>3</sup> )	Fine aggregate (kg/m <sup>3</sup> )	Water (kg/m <sup>3</sup> )	Silica fume (kg/m <sup>3</sup> )	SP (%)	W/C	Compressive strength (MPa)
H1 Series	460	910	825	168	40	0.5	0.37	82.0
H2 series	360	940	870	180	-	1	0.50	63.0
N Series	400	700	1100	152	-	1	0.38	38.2

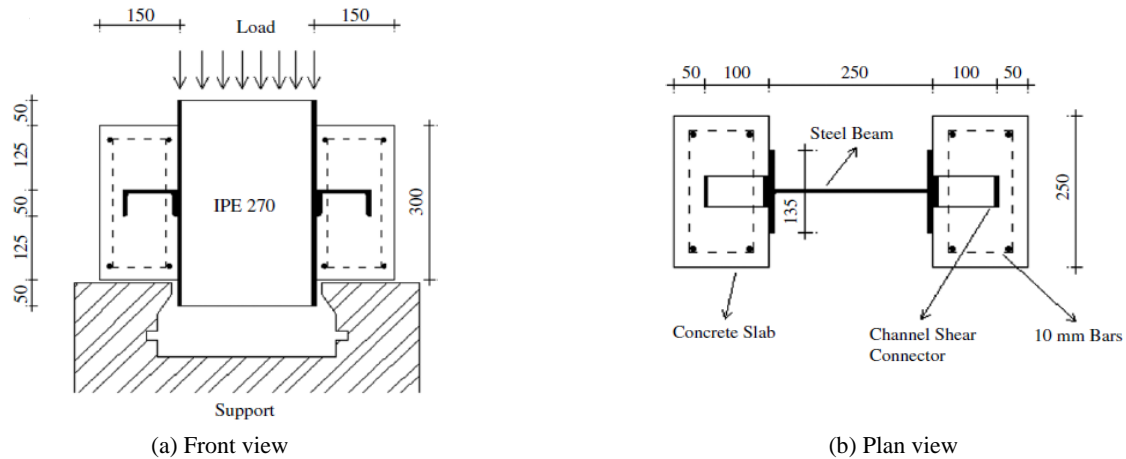


Fig. 1 Details of a typical push-out specimen

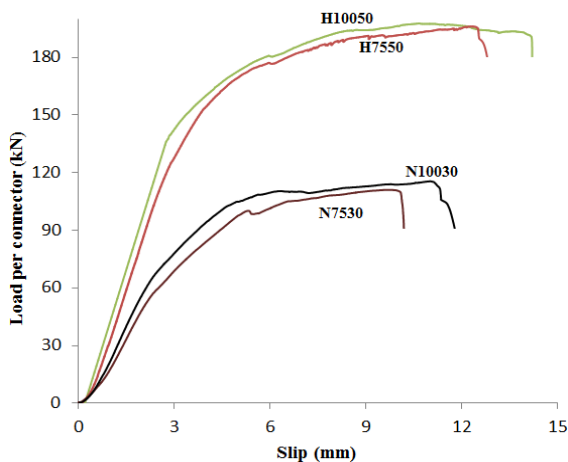


Fig. 2 The load-slip curve observed in the specimens under monotonic loading system

presented in Table 5.

In this study, the 1<sup>st</sup> letter represented the concrete type from its series such as the HSC denoted as H and the normal strength concrete indicated as N, while the 1<sup>st</sup> two digits indicated height and the last two/three digits designated length of the CSC in the concrete slabs (Fig. 1).

### 2.1.2 Loading and testing procedure

In this study, the load was employed using a universal testing machine (containing 600 kN capacity) and the specific support was applied only for loading the slabs. Loading control of 0.04 mm/s was used for loading rate of all specimens. The monotonic loading was involved for the loading system where a slow increment was experienced

until the failure.

During the present experiment, the I-beams (steel) were placed on the machine deck (universal machine). Variations in the orientation of the connector resulted from the variations of the ultimate strength related to the stiffness (Maleki and Bagheri 2008a) as presented in Fig. 1. During this investigation, practical loading with the relative slip of I-beam and concrete block were recorded automatically at each step by the test machine (universal machine).

## 2.2 Experimental test results

### 2.2.1 Failure type

The push-out specimens embedded either in the normal concrete or the HSC have demonstrated the channel fracture. The fracture was observed during the application of higher-strength concrete in the push-out test (Maleki and Bagheri 2008b). However, the load-slip curve (Fig. 2) was observed for the channel fracture at failure with a sudden end. The concrete strength and concrete failures determined the ultimate shear capacity of the connector. In this study, the load and compressive strength of concrete were followed as stated by Pashan (2006).

The channel fracture was observed in all specimens for the reinforcement. The channel failure was defined during the close contact of the channel and fracture to the bottom flange fillet (Maleki and Bagheri 2008a). A similar type of failure was observed for all specimens during the monotonic and cyclic loading.

### 2.2.2 Load-slip curve analysis

The strength (static strength) was observed to be an essential criterion for designing the shear connector where

the ductility confirmed throughout the ultimate slip (Shim 2004). Here, the curve (load-slip curve) was utilised for extracting the mechanical properties of the connector.

The slip took place in the middle of the I-beam and block during the monotonic and cyclic loading. However, from the static curve, it could be concluded that all channel connectors provided sufficient ductility in the HSC with larger slip ( $> 4$  mm). At the peak of the monotonic loading system, the relative slip was within 4 mm to 9 mm for all specimens. For this reason, the levels of HSC were not so essential for the ductility in the HSC. Hence, the curve illustrated that loading capacity was reduced quickly beyond the peak load with a sudden termination. Besides, all specimens had demonstrated a yield plateau.

## 2.3 Finite element analysis (FEA)

### 2.3.1 Introduction

In this study, a numerical model was developed using the finite element method for simulating the push-out test of the CSC focused on the capacity of connectors implanted in the normal and HSC slab during the monotonic loading procedure. During this test, all models were validated by the test, which was presented in the respective section (experiments and tests section). The parametric analysis was also conducted by using this nonlinear model for investigating variations in the connector dimensions and concrete strength of the specimen.

A detailed FEA was also employed to evaluate and compare the results of the push-out tests. The purpose of this part was the simulation of the push-out test results through finite element modelling as well as the investigation of the parameters, which were, affected the performance of the connectors through the parametric study. Results from the FEA and the parametric analysis could be utilized in an extensive verification of performance of the connector without resorting expensive tests (push-out tests). Besides, results from the parametric modelling could be employed for achieving certain output (results) that were not observed through the experiment. The objectives of the present study were fulfilled when an accurate modelling was designed by considering some parameters (nonlinear materials, geometries, concrete crushing, cracking, contact interaction) along with the suitable elements from steel and concrete. Moreover, accurate modelling should be capable of providing the appropriate solutions for the problematic convergence.

However, during the study, the specimens modelled in the FEA similar to specimens in the experiment and in the finite element program (ABAQUS 2011). The models had proved by the close values as obtained from the tests to predict the shear capacity. Therefore, effects of various parameters (height and length of shear connectors, flange thickness, web thickness, and concrete properties) could be predicted effectively from this model.

However, models from FEA were designed for matching with the specimens, which were developed from the parametric analysis and push-out test. This designed model was considered accurate only after adopting appropriate materials, mesh size, and an interface boundary condition. Thus, this calibrated model, as well as parametric analysis,

was performed for getting an equation to predict the capacity of the CSC embedded in the HSC.

## 2.3.2 Material properties

### 2.3.2.1 Steel

In this research, the kinematic bilinear relationship between the stress and strain was considered for the connectors and reinforcing bar in the concrete slab. The relation between the stress and strain for the steel materials is shown in Fig. 3(a). The Von Mises yield criterion for defining the associated flow rule and the material yield surface for determining the plastic deformation were used in this experiment. Here, the elasticity modulus was denoted as, the density as ( $\gamma$ ), and the Poisson ratio ( $\nu$ ) which represented the 205 GPa, 7800 kg/m<sup>3</sup>, and 0.3, respectively. Moreover, the ultimate strength, as well as the yield of the steel components, was measured from the steel coupon testing.

### 2.3.2.2 Concrete

In this experiment, the relationship between stress and strain was used to define the behavior of the concrete materials following the Standard (1992). However, an equivalent uniaxial curve was obtained from the nonlinear behavior of the concrete during compression (Fig. 3(b)).

The curve consisted of three parts (elastic range, nonlinear parabolic portion and descending slope) Where

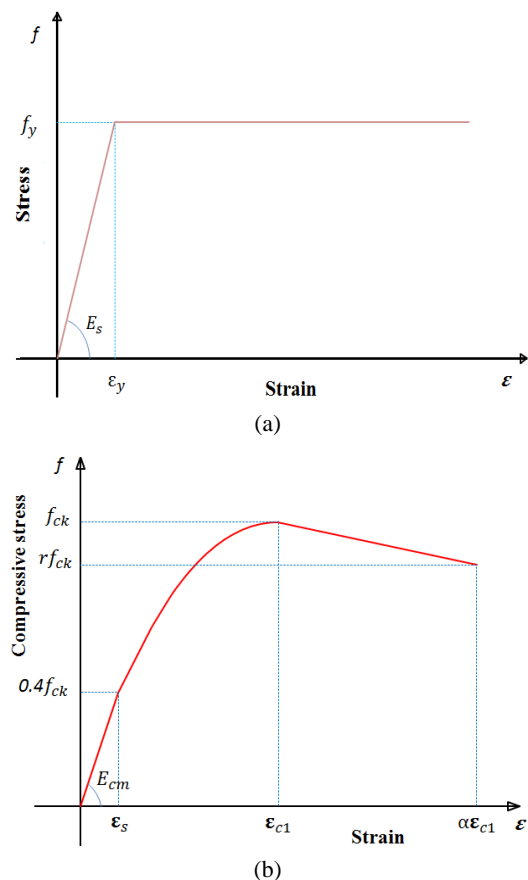


Fig. 3 Presentation of the relation between stress and strain for compression behavior of the steel (a); and concrete (b)

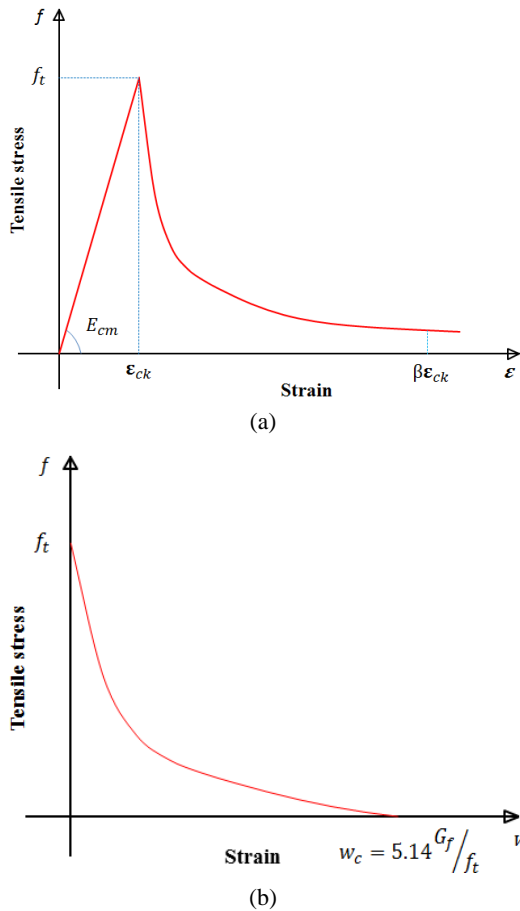


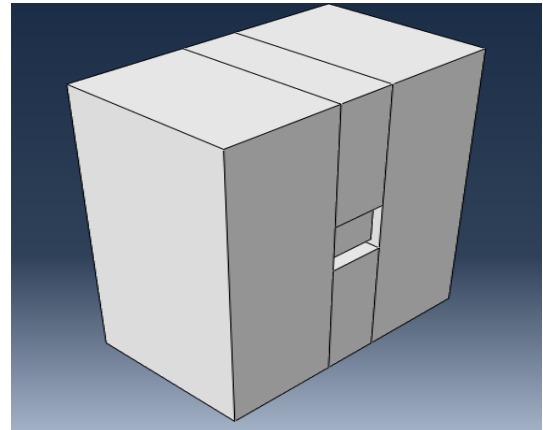
Fig. 4 Demonstration of the relation between stress and strain for the tensile behaviour of the concrete (a); and Exhibition of the exponential function of the tension softening model (b) (Cornelissen *et al.* 1986)

the 1<sup>st</sup> part was the proportional limit stress with the value of 0.4 (BSI 1992). The  $f_t$  was denoted for the strength of concrete in the cylinder specimen and expressed as the 0.8, where, the  $f_{cu}$  was the strength of cubic specimen. Here, strain  $\epsilon_{ck}$  value was as 0.0022 concerning the value. Therefore, the stress value for the nonlinear parabolic part could be obtained using Eqs. (1) and (2) (EUROCODE 2 2005) as follows.

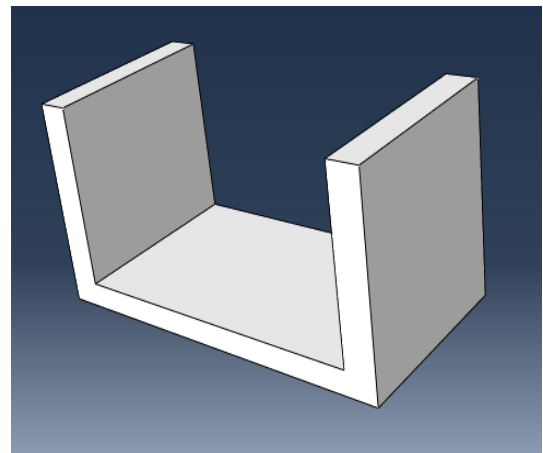
The descending part was employed for defining the post failure of the concrete compression behavior in specimens. In this experiment, the descending slope was ceased at a stress value of  $r$  where the  $r$  was symbolized for the reduction factor as stated by Ellobody and Young (2006). The range of  $r$  (1 to 0.5) corresponded to the strength of the cube (30 MPa to 100 MPa). Hence, an ultimate strain of the concrete at failure  $\epsilon_{cu}$  was defined as where was equivalent to 0.0035 as stated by the Standard (1992) and Structural Use of Concrete, Part 2 (1998), was equal to 1.75, density ( $\gamma$ ) and Poisson's ratio ( $\nu$ ) were assumed at 2.350 kg/m<sup>3</sup> and 0.2, respectively. Therefore, the elasticity module ( $E$ ) obtained from the Standard (1992) was similar to the Eq. (2).

However, nonlinear behavior of concrete in the tension is shown in Fig. 4 by using the uniaxial curve.

Tensile stress in concrete was increased linearly until the concrete cracks and then decreased to zero. However,



(a)



(b)

Fig. 5 The typical modelling of the specimens (a); and the steel part in the specimen (b)

cracking could be in three ways (linear, bilinear, and exponential) when there were no or only a few reinforcing bars existed in the concrete (ABAQUS 2011). In this experiment, the exponential function type (Cornelissen *et al.* 1986) was used for defining the tension softening curves. The tension existed in the stress and crack displacement relationship is shown in Fig. 4.

In this experiment, the model of concrete damage presumed by a non-associated potential plastic flow where the Drucker-Prager hyperbolic function was employed as the flow potential. Therefore, during this investigation, material dilation angle ( $\Psi$ ) was 35° and eccentricity ( $\epsilon$ ) was 0.1. The ratio of the strength of biaxial and uniaxial compressive was 1.16.

### 2.3.3 Modelling of the specimens

During modelling of the specimens, all components (connectors, bars, and slab) were modelled through the ABAQUS (2011) for obtaining an accurate result. During this experiment, the general contact was also activated to model the interaction of components. The modelling (interaction modelling) was the critical part in the analysis and required notable attention. The specimens consisted of similar geometry as described earlier, and the models (geometric model) consisted of three main parts (steel shear

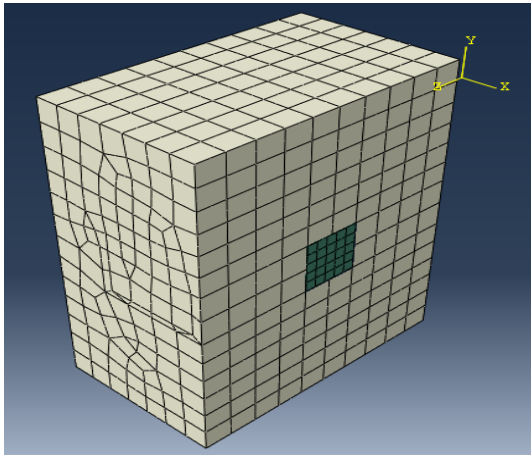


Fig. 6 Presentation of the typical finite element meshes of the concrete

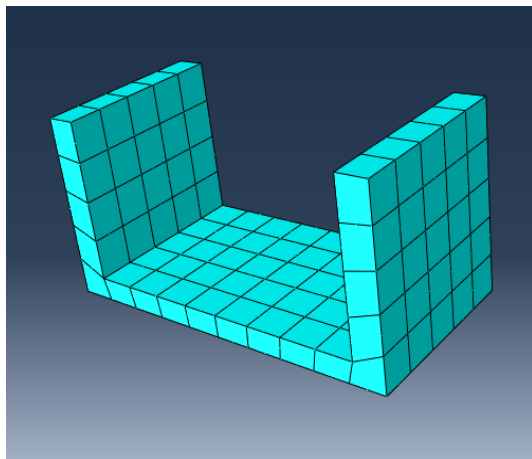


Fig. 7 Demonstration of the typical finite element meshes of the steel connector

connector, reinforcing bars, and concrete slab).

The typical specimen (parts in geometry) is shown in Fig. 5 while the steel parts modelled in software is shown in Fig. 5(b) separately.

### 2.3.4 Element type

The typical finite element mesh of the specimens to model the geometry of the test specimen is shown in Fig. 6 and Fig. 7. The accuracy and the computational time were considered during the mesh size selection. The element for the finite element modelling is as follows:

#### (1) Solid element:

About twenty-node in the solid element (C3D20R) were employed to model the connector and slab. Three translational degrees of freedom (3 df) at each node was applied for cracking in three orthogonal directions.

#### (2) Truss element:

To model the reinforcing bars, the truss element (T3D2) was used which also contained three translational df (translation in the  $x$ ,  $y$ , and  $z$  directions) at each node.

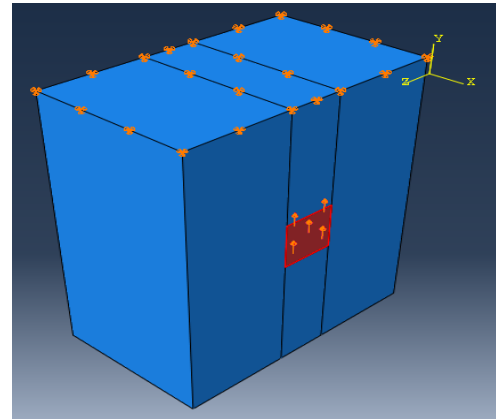


Fig. 8 The loading and boundary condition

After the election of the suitable elements, the discretization of each part constituting the model was made by applying a coarse mesh as an overall size to reduce the time of analysis. Then the fine mesh was applied in order to obtain more accurate results.

### 2.3.5 Element interaction

The FEA behavior relied upon the relationship among different parts. However, an interaction between bars and slab was expected to be completely bonded without the slip in the middle of them. Consequently, parts of the slab adjacent to the bars were used to assign the embedded element.

#### 2.3.5.1 Contact interaction

The contact between the concrete block and shear connector is an important modeling issue. In reality, when there is a compressive force between the concrete block and shear connector, the two elements act as one, otherwise they separate. To model this behavior, the penalty contact method is used. In this manner, the two surfaces act together in compression but separate in tension. The general contact was defined the interaction between the steel and concrete parts. The tangential contact was considered to define the friction between steel and concrete. In addition, the coefficient of friction associated with the penalty method is assumed to be 0.2.

### 2.3.6 Loading and boundary condition

Similar loading system was applied to the test specimen and the FEA while the vertical loading procedure was utilized for the slab. However, in both cases, the loading direction was downward as shown in Fig. 8.

The loading step was applied just after assembling different parts and only the linear loading system was employed for this analysis. The loading procedure was same for the experiment and push-out test but applied instantly. In the situation where the ultimate load could not be perceived during the parametric analysis, the maximum loading was 1.5 times of the real strength of any specimen. The final step was designed for obtaining the results of the parameters (stress, strain, and boundary condition). However, the time for analysis depended on the number of parameters.

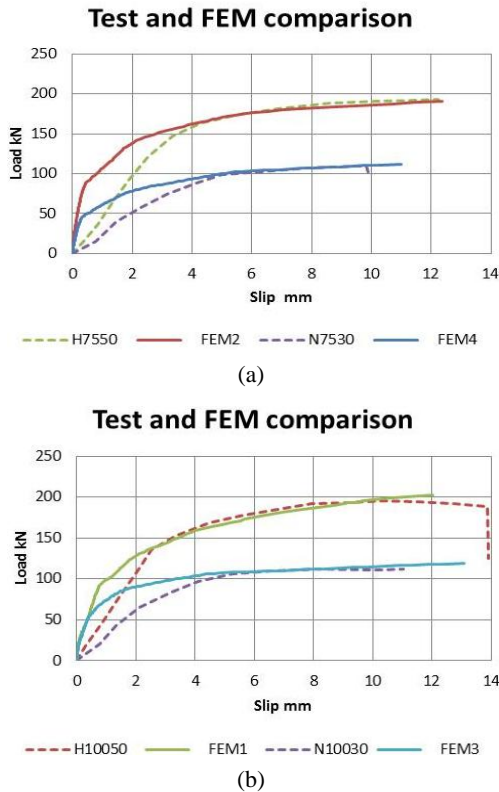


Fig. 9 Comparison of test results and FEM analysis for specimen N1007530 (a); and Comparison of test results and FEM analysis for specimen N10030 (b)

2.3.7 Analysis solution

In this investigation, initially, the general static of the ABAQUS standard was utilised. However, this type of initial analysis produced convergence problem and stopped the investigation. Similarly, the RIKS method also resulted in convergence problem in an initial analysis (Kim and Nguyen 2010). So, the explicit standard which applicable for nonlinear static analysis with large deformations and complicated interactions was applied for the present analysis. The ABAQUS Explicit was identified as a suitable method for analyzing the nonlinear materials, deformation, geometry, discontinuous parts, and concrete damage (ABAQUS 2011). The reduced integration, second accuracy, and enhanced control were also considered in the analysis for the solid element.

3. Results and discussions

3.1 Finite element results

The effective numerical analysis was proposed for simulating the push-out test. The motivation for the effective numerical analysis was defined as the prediction of the capacity of connectors in monotonic loading system. In this experiment, models were authenticated by the test results. Moreover, the parametric analysis was also performed using these nonlinear models for investigating the variations present in the connector dimensions and concrete strength.

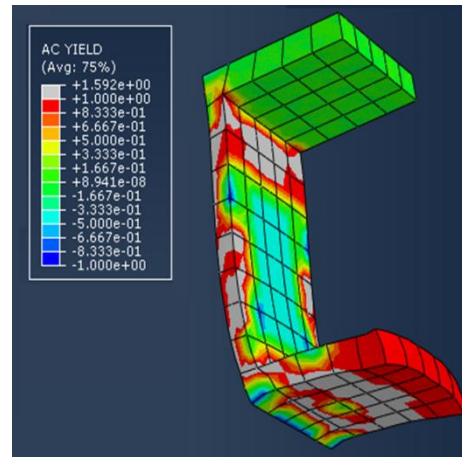


Fig. 10 The yield contours in the shear connector

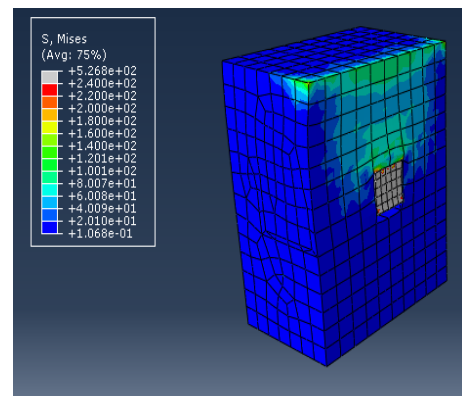


Fig. 11 The Von Mises contours in the steel and concrete

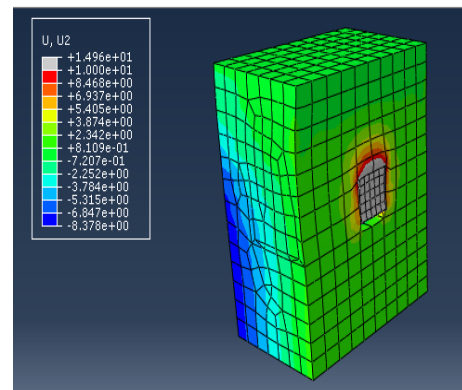


Fig. 12 The displacement in the y direction

3.1.1 Verification of the finite element results

Results from the finite element analysis were verified by the check to ensure an accuracy of modelling. The load–slip relationship is shown in Figs. 9(a) and (b) while a series of the typical Von Mises stress and plastic strains of the specimens are presented in Figs. 10 to 12. The FEA exhibited the accurate elastic and inelastic behaviour of the connections as presented in Table 6.

3.1.2 Parametric study for finite element method

In this investigation, the parametric analysis was

Table 6 The comparison of test results and the FEM analysis

Case	test	fem	error %
H7550	196.1	190.42	-2.9
N7530	111.1	111.77	0.6
H10050	197.7	202.61	2.48
N10030	115.5	119.28	3.27
C7550	139.7	136.26	-2.5
C7530	109.5	108.85	-0.6
C10050	152.5	153.86	0.89
C10030	112.3	111.76	-0.48

conducted to investigate the effects of various geometric properties of the connector and concrete strengths on shear capacity. However, capacities of the CSC obtained from the FEA were evaluated and discussed only after verifying the results from the finite element against the test. Hence, the discussion was deliberated mostly on the capacity alterations using monotonic loading. Here, the dimensions of the connector and types of the concrete were also considered. The capacity of the CSC in the FEA was also measured and summarized in Table 7.

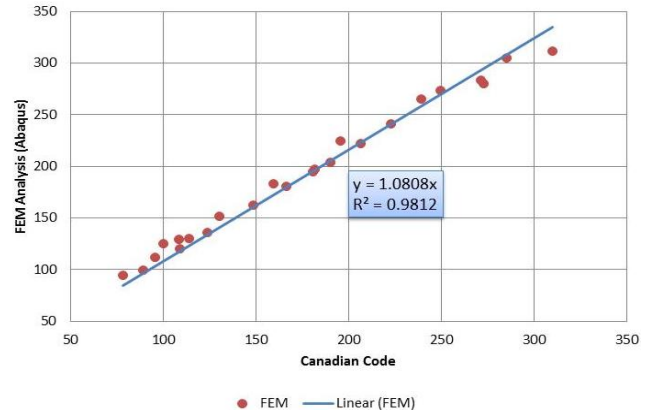


Fig. 13 The capacity from the FE analysis versus the Canadian code

### 3.1.3 Evaluation of current design codes

The failure (static failure) was measured from the peak of the curve and presented in Table 7. These values (failure values) were matched with the ultimate capacity (Eq. (1)) and relative strength of the channel connector as presented in Table 7. The equation one (Eq. (1)) was obtained from the reinforced push-out tests using the monotonic loading system (Maleki and Bagheri 2008b). However, the validity

Table 7 The parametric study of shear connectors and the FEM results

Specimen	$F_c$ (Mpa)	$h$ (mm)	$b$ (mm)	$tw$ (mm)	$tf$ (mm)	$L$ (mm)	Canadian Code	FE results	Difference ratio
H60L30F82	82	60	30	6	6	30	89.24	99.85	10.62%
H60L50F82						50	148.73	162.21	8.31%
H60L75F82						75	223.10	241.47	7.61%
H80L30F82		80	45	6	8	30	109.07	120.42	9.42%
H80L50F82						50	181.79	197.46	7.94%
H80L75F82						75	272.68	280.60	2.82%
H100L30F82		100	50	6	8.5	30	114.03	130.23	12.44%
H100L50F82						50	190.05	203.90	6.79%
H100L75F82						75	285.07	304.65	6.43%
H120L30F82	120	55	7	9	30	123.95	136.36	9.10%	
H120L50F82					50	206.58	222.20	7.03%	
H120L75F82					75	309.86	312.10	0.72%	
H60L30F63	63	60	30	6	6	30	78.22	94.45	17.18%
H60L50F63						50	130.37	151.56	13.98%
H60L75F63						75	195.55	225.00	13.09%
H80L30F63		80	45	6	8	30	95.60	111.74	14.44%
H80L50F63						50	159.34	183.47	13.15%
H80L75F63						75	239.01	265.34	9.92%
H100L30F63		100	50	6	8.5	30	99.95	125.54	20.38%
H100L50F63						50	166.58	180.58	7.75%
H100L75F63						75	249.87	273.90	8.77%
H120L30F63	120	55	7	9	30	108.64	129.10	15.84%	
H120L50F63					50	181.07	195.06	7.17%	
H120L75F63					75	271.60	283.26	4.12%	

of this equation (Eq. (1)) was not determined in other conditions but from Table 7, it can be perceived that the strength prediction from the NBC code was not suitable for the FEM. However, in HSC, this formula was observed to be less effective for predicting the shear strength of connectors due to the higher FEM strength of CSC than the Canadian code strength.

Fig. 13 is representing straight line for fitted data with a reasonable accuracy. The slope of this line was 1.081 which was greater than one ( $1.081 > 1.000$ ) indicated the suitability of the code for predicting the capacity of CSC embedded in the HSC. Hence, the coefficient of 1.081 in the code's equation one (Eq. (1)) could provide a better estimate of the capacity in the HSC. However, the Equation 4 was the modified code equation (Eq. (1)) which was applied to estimate the shear capacity of the channels surrounded in the HSC. The standard deviation (SD) value was 2.88 and the suggested equation is as follows

$$Q_n = 39.45 \times (t_f + 0.5t_w) \times L_c \times \sqrt{f_c} \quad (2)$$

#### 4. Conclusions

In this experiment, a limited push-out test revealed the behaviour of the CSC placed in an HSC slab under monotonic loading system. The push-out test was also conducted to evaluate the efficacy of the NBC for estimating the loading capacities of the channel connectors. The main result represented that the NBC code was not suitable for the strength prediction of all specimens. Therefore, the formula from NBC code was less effective for predicting the shear strength of connectors in the HSC because of the higher experimental strength than the Canadian code strength. Through this investigation, a model was proposed using the ABAQUS software for predicting the push-out test values. A parametric study was also performed for estimating the sizes of connectors surrounded in the HSC. However, the capacity of these connectors was 1.081% accurate than the accuracy predicted by the Canadian code equation. Thus, modification of the equation from the Canadian code is required for the capability estimation of the channel connectors embedded in the HSC. The modified equation was proposed as mentioned above.

#### References

- ABAQUS, A.S. (2011), User's manual, Version 6.11. 1; Dassaults Systemes Inc.
- Abedini, M., Khlaghi, E.A., Mehrmashhadi, J., Mussa, M.H., Ansari, M. and Momeni, T. (2017), "Evaluation of Concrete Structures Reinforced with Fiber Reinforced Polymers Bars: A Review", *J. Asian Sci. Res.*, **7**(5), 165-175.
- AISC (2005), Specification for structural steel buildings, American Institute of Steel Construction Inc., Chicago, IL, USA.
- Akgul, M., Demir, M. and Akay, A.E. (2017), "Analyzing dynamic curve widening on forest roads", *J. Forest. Res.*, **28**(2), 411-417.
- Andalib, Z. (2011), *Experimental and Numerical Investigation on the Ductility of Steel Ring Constructed from Steel Plates in Concentric Braces*, Semnan University, Iran.
- Andalib, Z., Kafi, M.A. and Bazzaz, M. (2010), "Using Hyper Elastic Material for Increasing Ductility of Bracing", *Proceedings of the 1st Conference of Steel & Structures and 2nd Conference on Application of High-Strength Steels in Structural Industry, Steel & Structures*.
- Andalib, Z., Kafi, M.A., Kheyroddin, A. and Bazzaz, M. (2011), "Investigation on the Ductility and Absorption of Energy of Steel Ring in Concentric Braces", *Proceedings of the 2nd Conference of Steel and Structures, Steel and Structures*.
- Andalib, Z., Kafi, M.A., Kheyroddin, A. and Bazzaz, M. (2014), "Experimental investigation of the ductility and performance of steel rings constructed from plates", *J. Constr. Steel Res.*, **103**, 77-88.
- Andalib, Z., Kafi, M.A., Bazzaz, M. and Momenzadeh, S. (2018), "Numerical evaluation of ductility and energy absorption of steel rings constructed from plates", *Eng. Struct.*, **169**, 94-106.
- ASTM C39 / C39M-04 (2004), Standard test method for compressive strength of cylindrical concrete specimens, ASTM International, West Conshohocken, PA, USA.
- Awal, A.A., Shehu, I.A. and Ismail, M. (2015), "Effect of cooling regime on the residual performance of high-volume palm oil fuel ash concrete exposed to high temperatures", *Constr. Build. Mater.*, **98**, 875-883.
- Ayatollahi, M.R., Mirsayar, M.M. and Dehghany, M. (2011), "Experimental determination of stress field parameters in bi-material notches using photoelasticity", *Mater. Des.*, **32**(10), 4901-4908.
- Baran, E. and Topkaya, C. (2012), "An experimental study on channel type shear connectors", *J. Constr. Steel Res.*, **74**, 108-117.
- Baran, E. and Topkaya, C. (2014), "Behavior of steel-concrete partially composite beams with channel type shear connectors", *J. Constr. Steel Res.*, **97**, 69-78.
- Bazzaz, M. (2010), *Seismic Behavior of Off-Centre Braced Frame with Circular Element in Steel Frame Design*, Semnan University.
- Bazzaz, M., Kheyroddin, A., Kafi, M.A. and Andalib, Z. (2011a), "Evaluating the performance of steel ring in special bracing frame", *Proceedings of the 6th Seismology and Earthquake Engineering International Conference*, Ministry of Science, Research and Technology.
- Bazzaz, M., Kafi, M.A., Andalib, Z. and Esmaeili, H. (2011b), "Seismic Behavior of Off-centre Bracing Frame", *Proceedings of the 6th National Congress on Civil Engineering*.
- Bazzaz, M., Kheyroddin, A., Kafi, M.A. and Andalib, Z. (2012a), "Evaluation of the seismic performance of off-centre bracing system with ductile element in steel frames", *Steel Compos. Struct., Int. J.*, **12**(5), 445-464.
- Bazzaz, M., Kheyroddin, A., Kafi, M.A. and Andalib, Z. (2012b), "Modeling and Analysis of Steel Ring Devised in Off-centric Braced Frame with the Goal of Improving Ductility of Bracing Systems", Iran Scientific and Industrial Researches Organization, Tehran, Iran.
- Bazzaz, M., Kafi, M.A., Kheyroddin, A., Andalib, Z. and Esmaeili, H. (2014), "Evaluating the seismic performance of off-centre bracing system with circular element in optimum place", *Int. J. Steel Struct.*, **14**(2), 293-304.
- Bazzaz, M., Andalib, Z., Kafi, M.A. and Kheyroddin, A. (2015a), "Evaluating the performance of OBS-C-O in steel frames under monotonic load", *Earthq. Struct., Int. J.*, **8**(3), 697-710.
- Bazzaz, M., Andalib, Z., Kheyroddin, A. and Kafi, M.A. (2015b), "Numerical comparison of the seismic performance of steel rings in off-centre bracing system and diagonal bracing system", *Steel Compos. Struct., Int. J.*, **19**(4), 917-937.
- Bozorgzad, A. and Lee, H.D. (2017), "Consistent distribution of air voids and asphalt and random orientation of aggregates by flipping specimens during gyratory compaction process",

- Constr. Build. Mater.*, **132**, 376-382.
- BS 1881 (1983), "Testing Concrete, Part 121, 'Method for the Determination of Compressive Strength of Concrete Cores', British Standards Institution, London, UK.
- BSI, B.B.S.I. (1983), Method for determination of the compressive strength of cores, Part 120, London, UK.
- BSI, B. (1992), Concrete performance, production, placing and compliance criteria. DD ENV 206:1992. London.
- Cement, A.P. (1993), "ASTM C 150, Type I or II, except Type III may be used for cold-weather construction", Provide natural color or white cement as required to produce mortar color indicated 1.
- Cornelissen, H.A.W., Hordijk, D.A. and Reinhardt, H.W. (1986), "Experimental determination of crack softening characteristics of normalweight and lightweight concrete", *HERON*, **31**(2), 1986.
- Ellobody, E. and Young, B. (2006), "Performance of shear connection in composite beams with profiled steel sheeting", *J. Constr. Steel Res.*, **62**(7), 682-694.
- Eslami, M. and Namba, H. (2016a), "Elasto-plastic behavior of composite beam connected to RHS column, experimental test results", *Int. J. Steel Struct.*, **16**(3), 901-912.
- Eslami, M. and Namba, H. (2016b), "Mechanism of elasto-plastic behavior of composite beam connected to RHS column", *Int. J. Steel Struct.*, **16**(3), 913-933.
- Eslami, M. and Namba, H. (2016c), "Rotation capacity of composite beam connected to RHS column, experimental test results", *Steel Compos. Struct., Int. J.*, **22**(1), 141-159.
- EUROCODE 2 (2005), EN 1992-1-1; Design of concrete structures Part 1.1 General rules and rules for buildings. CEN-European Committee for Standardisation, Brussels, Belgium.
- Fanaie, N., Esfahani, F.G. and Soroushnia, S. (2015), "Analytical study of composite beams with different arrangements of channel shear connectors", *Steel Compos. Struct., Int. J.*, **19**(2), 485-501.
- Farzad, M., Mohammadi, A., Shafieifar, M., Pham, H. and Azizinamini, A. (2017), "Development of Innovative Bridge Systems Utilizing Steel-Concrete-Steel Sandwich System".
- Haji Agha Mohammad Zarbaf, S.E., Norouzi, M., Allemang, R.J., Hunt, V.J. and Helmicki, A. (2017a), "Stay cable tension estimation of cable-stayed bridges using genetic algorithm and particle swarm optimization", *J. Bridge Eng.*, **22**(10), 05017008.
- Haji Agha Mohammad Zarbaf, S.E., Norouzi, M., Allemang, R.J., Hunt, V.J., Helmicki, A. and Nims, D.K. (2017b), "Stay force estimation in cable-stayed bridges using stochastic subspace identification methods", *J. Bridge Eng.*, **22**(9), 04017055.
- Heydari, A. (2011), "Buckling of Functionally Graded Beams with Rectangular and Annular Sections Subjected to Axial Compression", *Int. J. Adv. Des. Manuf. Technol.*, **5**(1).
- Heydari, A. and Shariati, M. (2018), "Buckling analysis of tapered BDFGM nano-beam under variable axial compression resting on elastic medium", *Struct. Eng. Mech., Int. J.*, **66**(6).
- Hosain, M.U. and Pashan, A. (2006), *Channel Shear Connectors in Composite Beams: Push-Out Tests*, Kruger National Park, Berg-en-Dal, Mpumalanga, South Africa, ASCE.
- Hosain, M. and Pashan, A. (2009), "New design equations for channel shear connectors in composite beams", *Can. J. Civil Eng.*, **36**, 1435-1443.
- Kazemi, M.T., Momenzadeh, S.-B. and Hoseinzadehasl, M. (2012), "Study of reduced beam section connections with web opening", *Proceedings of the 15th World Conference on Earthquake Engineering*, Lisbon, Portugal, September.
- Kim, S.E. and Nguyen, H.T. (2010), "Finite element modeling and analysis of a hybrid steel-PSC beam connection", *Eng. Struct.*, **32**(9), 2557-2569.
- Kodur, V., Yahyai, M., Rezaeian, A., Eslami, M. and Poormohamadi, A. (2017), "Residual mechanical properties of high strength steel bolts subjected to heating-cooling cycle", *J. Constr. Steel Res.*, **131**, 122-131.
- Maleki, S. and Bagheri, S. (2008a), "Behavior of channel shear connectors, Part I: Experimental study", *J. Constr. Steel Res.*, **64**, 1333-1340.
- Maleki, S. and Bagheri, S. (2008b), "Behavior of channel shear connectors, Part II: Analytical study", *J. Constr. Steel Res.*, **64**, 1341-1348.
- Maleki, S. and Mahoutian, M. (2009), "Experimental and analytical study on channel shear connectors in fiber-reinforced concrete", *J. Constr. Steel Res.*, **65**(8-9), 1787-1793.
- Mohammadhassani, M., Nezamabadi-Pour, H., Suhatri, M. and Shariati, M. (2013), "Identification of a suitable ANN architecture in predicting strain in tie section of concrete deep beams", *Struct. Eng. Mech., Int. J.*, **46**(6), 853-868.
- Momenzadeh, S.B. (2012), "Performance of Circular Opening in Beam Web Connections", *Life Sci. J.*, **9**(3), 1377-1383.
- Momenzadeh, S. and Shen, J. (2018), "Seismic demand on columns in special concentrically braced frames", *Eng. Struct.*, **168**, 93-107.
- Momenzadeh, S., Seker, O. and Shen, J. (2017a), "Observed seismic demand on columns in SCBFs", *AEI 2017*, 647-658.
- Momenzadeh, S., Seker, O., Faytarouni, M. and Shen, J. (2017b), "Seismic performance of all-steel buckling-controlled braces with various cross-sections", *J. Constr. Steel Res.*, **139**, 44-61.
- Momenzadeh, S., Kazemi, M.T. and Asl, M.H. (2017c), "Seismic performance of reduced web section moment connections", *Int. J. Steel Struct.*, **17**(2), 413-425.
- NBC (2005), National Building Code of Canada.
- Pashan, A. (2006), "Behaviour of channel shear connectors: push-out tests", M.S. Thesis; Department of Civil Engineering, University of Saskatchewan, Canada.
- Rassouli, B., Shafaei, S., Ayazi, A. and Farahbod, F. (2016), "Experimental and numerical study on steel-concrete composite shear wall using light-weight concrete", *J. Constr. Steel Res.*, **126**, 117-128.
- Razak, H.A. and Sajedi, F. (2011), "The effect of heat treatment on the compressive strength of cement-slag mortars", *Mater. Des.*, **32**(8-9), 4618-4628.
- Safa, M., Shariati, M., Ibrahim, Z., Togholi, A., Baharom, S.B., Nor, N.M. and Petkovic, D. (2016), "Potential of adaptive neuro fuzzy inference system for evaluating the factors affecting steel-concrete composite beam's shear strength", *Steel Compos. Struct., Int. J.*, **21**(3) 679-688.
- Sajedi, F. and Abdul Razak, H. (2010), "Thermal activation of ordinary Portland cement-slag mortars", *Mater. Des.*, **31**(9), 4522-4527.
- Sajedi, F. and Razak, H.A. (2011), "Effects of thermal and mechanical activation methods on compressive strength of ordinary Portland cement-slag mortar", *Mater. Des.*, **32**(2), 984-995.
- Shafaei, S., Ayazi, A. and Farahbod, F. (2016), "The effect of concrete panel thickness upon composite steel plate shear walls", *J. Constr. Steel Res.*, **117**, 81-90.
- Shafaei, S., Farahbod, F. and Ayazi, A. (2017), "Concrete Stiffened Steel Plate Shear Walls With an Unstiffened Opening", *Structures*, **12**, 40-53.
- Shafaei, S., Farahbod, F. and Ayazi, A. (2018), "The wall-frame and the steel-concrete interactions in composite shear walls", *Struct. Des. Tall Special Build.*, e1476.
- Shafieifar, M., Azizinamini, A. and Director, A. (2016), "Alternative ABC Connections Utilizing UHPC".
- Shafieifar, M., Farzad, M. and Azizinamini, A. (2017), "Experimental and numerical study on mechanical properties of Ultra High Performance Concrete (UHPC)", *Constr. Build. Mater.*, **156**, 402-411.

- Shahabi, S., Sulong, N., Shariati, M., Mohammadhassani, M. and Shah, S. (2016), "Numerical analysis of channel connectors under fire and a comparison of performance with different types of shear connectors subjected to fire", *Steel Compos. Struct., Int. J.*, **20**(3), 651-669.
- Shariati, M., Ramli Sulong, N.H., Sinaei, H., Arabnejad Kh, M.M. and Shafiqh, P. (2010), "Behavior of Channel Shear Connectors in Normal and Light Weight Aggregate Concrete (Experimental and Analytical Study)", *Adv. Mater. Res.*, **168-170**, 2303-2307.
- Shariati, M., Sulong, N.H.R., KH, M.M.A. and Mahoutian, M. (2011), "Shear resistance of channel shear connectors in plain, reinforced and lightweight concrete", *Sci. Res. Essays*, **6**(4), 977-983.
- Shariati, M., Ramli Sulong, N.H. and Arabnejad Khanouki, M.M. (2012a), "Experimental assessment of channel shear connectors under monotonic and fully reversed cyclic loading in high strength concrete", *Mater. Des.*, **34**, 325-331.
- Shariati, A., Sulong, N.R., Suhatrik, M. and Shariati, M. (2012b), "Investigation of channel shear connectors for composite concrete and steel T-beam", *Int. J. Phys. Sci.*, **7**(11), 1828-1831.
- Shariati, M., Ramli Sulong, N.H., Shariati, A. and Kueh, A.B.H. (2016), "Comparative performance of channel and angle shear connectors in high strength concrete composites: An experimental study", *Constr. Build. Mater.*, **120**, 382-392.
- Shen, J., Seker, O., Akbas, B., Seker, P., Momenzadeh, S. and Faytarouni, M. (2017), "Seismic performance of concentrically braced frames with and without brace buckling", *Eng. Struct.*, **141**, 461-481.
- Shim, C. (2004), "Experiments on limit state design of large stud shear connectors", *KSCE J. Civil Eng.*, **8**(3), 313-318.
- Standard, B. (1992), "Specification for aggregates from natural sources for concrete", London, BSI, 1-9.
- Structural Use of Concrete, Part 2 (1998), Code of Practice for Special Circumstances BS 8110: Part 2: 1997, British Standard Institution, London, UK.
- Toghroli, A., Mohammadhassani, M., Suhatrik, M., Shariati, M. and Ibrahim, Z. (2014), "Prediction of shear capacity of channel shear connectors using the ANFIS model", *Steel Compos. Struct., Int. J.*, **17**(5), 623-639.
- Toghroli, A., Darvishmoghaddam, E., Zandi, Y., Parvan, M., Safa, M., Abdullahi, M.a.M., Heydari, A., Wakil, K., Gebreel, S.A.M. and Khorami, M. (2018), "Evaluation of the parameters affecting the Schmidt rebound hammer reading using ANFIS method", *Comput. Concrete, Int. J.*, **21**(5), 525-530.